NOVEL PHENOMENA IN ENCAPSULATING HYDROCARBON GASES

by

ANAS W. SALEH

Presented to the Faculty of the Graduate School of

The University of Texas at Arlington in Partial Fulfillment

of the Requirements

for the Degree of

MASTER OF SCIENCE IN CHEMISTRY

THE UNIVERSITY OF TEXAS AT ARLINGTON

December 2007

ACKNOWLEDGEMENTS

During the course of my research, I have developed many skills. I learned that team work is an important aspect of any successful group. I learned that, even when working on your project independently, professor, lab mates, and post docs had a great impact on me and my learning process. I would like to acknowledge my research advisor Dr. Dmitry M. Rudkevich on his great support and passions for me in the lab. He was definitely a great help to me and my learning process. I would also like to thank my lab members on their help and support especially Dr. Leontiev.

I came to the University of Texas at Arlington fall of 2005 and have spent a great deal of my time interacting with students, staff, and faculty. They all have been great to me and in turn I would like to acknowledge them. And last but not least, I would like to specially acknowledge Dr. Carl J. Lovely, for all he has done for me, before, and after I arrived at UTA.

October 20, 2007

ABSTRACT

NOVEL PHENOMENA IN ENCAPSULATING HYDROCARBON GASES

Publication No. _____

Anas W. Saleh, M. S.

The University of Texas at Arlington, 2007

Supervising Professor: Dmitry Rudkevich (deceased August 4th 2007)

The use of hydrophobic forces for entrapment of gases in water will be discussed. Natural hydrocarbons, haloalkanes, and anesthetic gases are hydrophobic in nature. In the course of this investigation water-soluble molecular capsules that possess hydrophobic interiors were synthesized. The encapsulation of hydrocarbon gases in water and in solid state was achieved and monitored by NMR spectroscopy. Our findings may lead to novel, capsule-based materials for gas separation and purification.

The work presented in this thesis is divided into two sections. The first section discusses the synthesis of two water soluble hemicarcerands and their use as hosts in encapsulating hydrocarbon gases in water. These systems utilize hydrophobic interactions as the driving force in the encapsulation process. Both of the synthesized

hemicarcerands show the ability to encapsulate hydrocarbon gases in water. The encapsulation of the gases was monitored using ^{1}H NMR.

The second project discusses the encapsulation of hydrocarbon gases using solid state materials. It was found that traditional hemicarcerands are able to encapsulate gases in their solid-state. Therefore solid hemicarcerand **4** was tested for gas encapsulation. As expected, hemicarcerand **4** did show encapsulation of butane when flushed in the solid-state. Therefore hemicarcerand **4** was used as a monomeric unit in the synthesis of the first cavity-containing polymer. The polymer was tested for gas encapsulation.

TABLE OF CONTENTS

LIST OF FIGURES

LIST OF SCHEMES

CHAPTER 1

INTRODUCTION

Gases occupy the atmosphere of our planet. They also make up a central position in biomedicine, science, technology, and agriculture. For example, H_2 is extremely promising in the design of energy rich fuel cell devices.[5] N_2 is useful in space technology and in ammonia production.[3] O_2, CO_2, Cl_2 gases are utilized in chemical and medical industry.[9] Natural hydrocarbon gases are important energy sources. Some of these gases are greenhouse gases that are harmful to the environment. While others are blood gases that are essential to our well being. Chemical sensing, storage, separation and utilization of gases is now attracting a lot of attention.[16] We employ supramolecular chemistry for these purposes.

Supramolecular chemistry is the area of chemistry that focuses on the non-covalent bonding interactions between molecules.[1] Supramolecular chemistry utilizes fairly weak and reversible non-covalent interactions in the formation of multi-molecular complexes. Examples of such weak interactions are: hydrogen bonding, hydrophobic forces, van der Waals, π-π interactions and electrostatic effect.[2] Gas encapsulation is a new phenomenon that is still at its infancy stage.[3,4] From the literature, there are only a handful of examples in which gases can be encapsulated.[17]

Metal-organic frameworks (MOFs) use organic bridges to connect metal ions which will lead to the assembly of porous solids.[5] The cavities within MOFs are usually filled with solvent molecules. Permanent porosity is achieved upon removing the solvent

species. However, the possibility of collapsing occurs upon the removal of the solvent molecule is serious, which makes it a major drawback. Another drawback of MOFs is the need to employ relatively high pressure for gas encapsulation and storage. Other structures involve self-assembling capsules[6] and solid-state calix[4]arene lattices.[7] However, the need for a delicate environment in order to assemble represents a major drawback in the use of such cavities in a practical way. Such environments include the need for a specific concentration or a temperature range or else the assembled capsule falls apart.

Therefore, more stable hollow cavities are needed. Some time ago, Cram and co-workers synthesized robust and stable, covalently linked capsules called hemicarcerands. However, there was not sufficient driving force for the gases to be encapsulated in traditional hemicarcerands; the only forces of encapsulation used are weak van der Waals interactions. Therefore, the goal of this project was the design and synthesis of cavity containing molecules that utilize stronger forces, such as solvation and the hydrophobic effect, for gas encapsulation.

In chapter 2 of this manuscript, the design and synthesis of two water soluble hemicarcerand capsules and their gas encapsulation properties in water is discussed. In chapter 3, the synthesis of the first capsule bearing polymer and its gas encapsulating properties are discussed. All gases used were hydrocarbon gases ranging from methane to butane (C_1-C_4).[8,9] The final chapter will contain the experimental details and supporting information.

CHAPTER 2

GAS ENCAPSULATION IN WATER

2.1 Background

As stated earlier, gas encapsulating cavities such as self-assembled capsules are well known. The two portions of the capsule are joined using hydrogen bonding or the hydrophobic effect. Gibb et al. has demonstrated the encapsulation of hydrocarbon gases into a self-assembled capsule using the hydrophobic effect (Fig. 2.1).[9] However, the drawbacks from using such system for gas encapsulation are the same as any other self-assembled capsule.

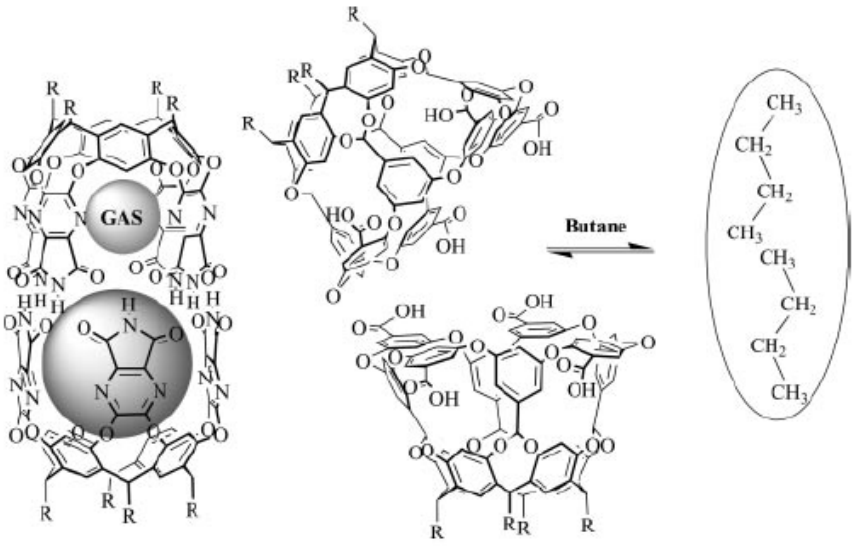

17 R = *n*-$C_{11}H_{23}$ **18** R = $CH_2CH_2C(O)OH$

Figure 2.1 Example of Self-assembled Capsule.[9]

In this study, we demonstrate that our robust hydrophobic cavities may encapsulate hydrophobic gases in water even without intrinsic affinity towards them. To simply illustrate this concept, commercially available hydrocarbon natural gases and hexaacid hemicarcerand **4** and octaacid hemicarcerand **8** were used.

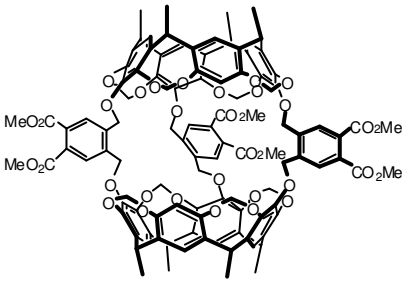

3

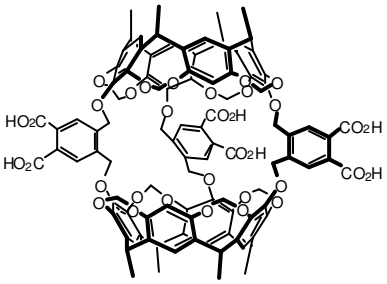

4

It was found that neither hemicarcerand **3** nor **7** have encapsulated methane, ethane, propane, and butane in $CDCl_3$ solution. This is explained by the movement of the gases in and out of the cavity through the widely open portals. In aqueous solution, however, the situation has changed. Water soluble hemicarcerands **4** and **8** showed an affinity to hydrocarbon gases.

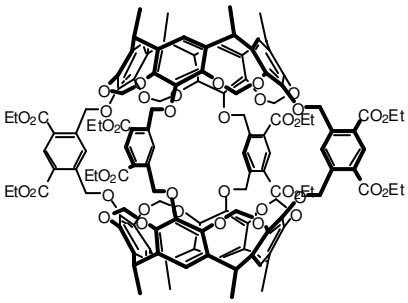

7

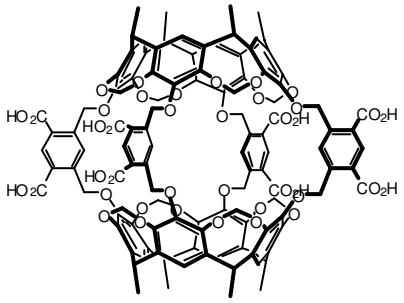

8

2.2 Hexaacid Hemicarcerand

To synthesize water soluble hemicarcerand **4**, hydroxyl cavitand **1**[10] was reacted with dibromide **2**[11] in dimethylacetamide (DMA) in the presence of Cs_2CO_3 to afford hemicarcerand **3**. The reaction took place under high dilution conditions because six covalent bonds are made simultaneously five of which result from intramolecular reactions. This, however, leads to lower yields. A hydrolysis reaction was used to convert the ester groups to carboxylic acids. This reaction takes place by reacting **3** with potassium hydroxide in the presence of 18-crown-6. After the removal of the organic layer solid **4** was obtained by adding 1 M HCl to the mixture. Upon the addition of a small amount of NaOH (~ pH 9), the deprotonation of the acid groups results in the formation of a water soluble salt, **4** (Scheme 2.1).

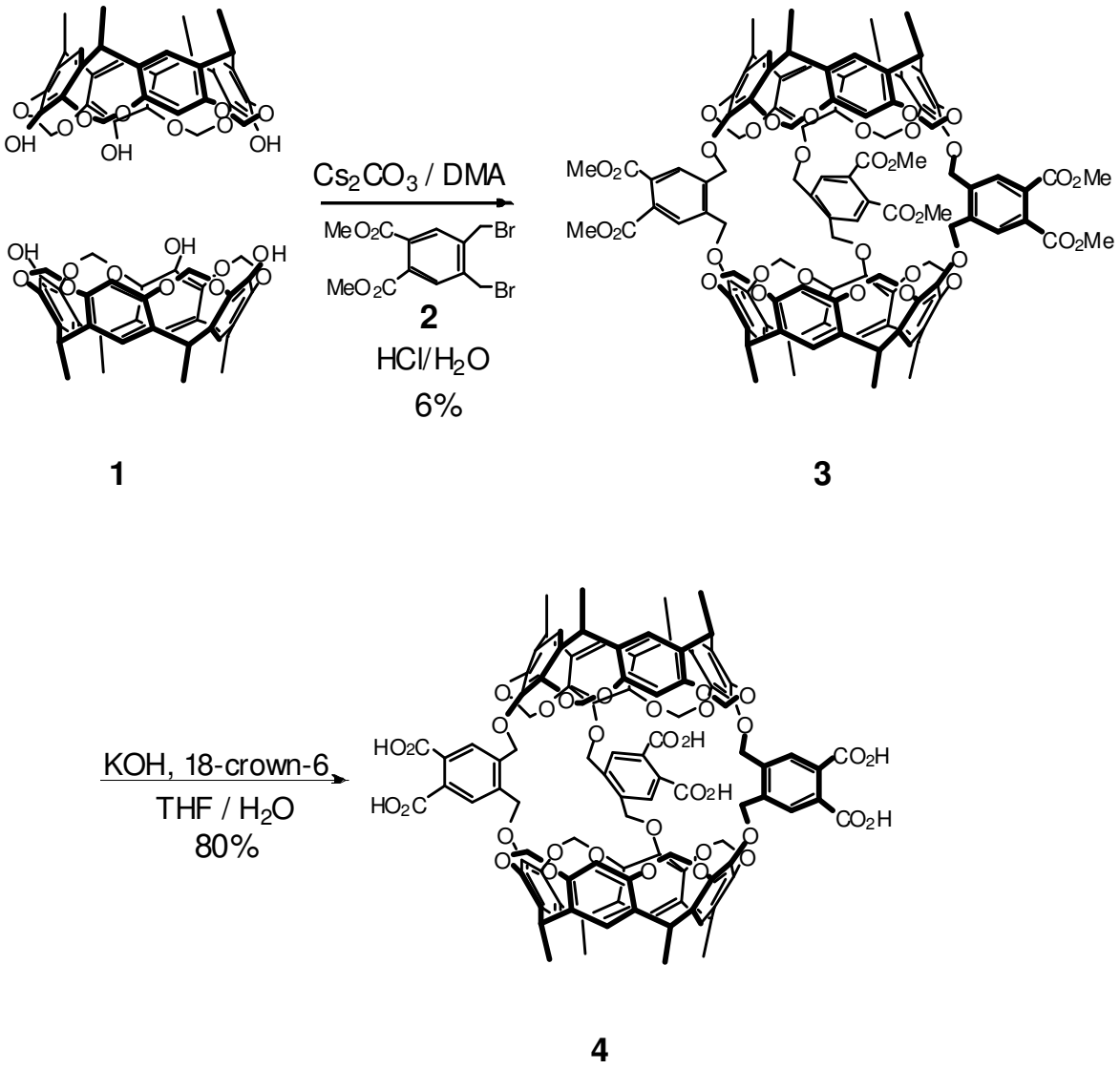

Scheme 2.1 The synthesis of water soluble trihemicarcerand **4**

As can be seen in figure 2.2 on the next page, new peaks begin to appear upon the encapsulation of methane in **4** at -0.10 ppm. Encapsulated ethane showed a broad peak around -0.19 ppm. Encapsulated propane showed two peaks, first peak at -1.06 ppm and second peak at -2.60 ppm. Encapsulated butane also showed two peaks: first peak at -1.12 ppm and second peak at -3.37 ppm. However, when natural gas was bubbled through a solution of **4**, the encapsulation of methane, propane, and butane was observed. One can notice that the shapes of the peaks obtained for all cases were broad and do not have a fine structure. This can be explained by the uniform movement of the gas in and out of the cavity at a high speed.

Another experiment was done on the system using a isobutane instead of butane. Similar results as above were obtained. Two peaks appeared in the spectrum; the first peak is a singlet at -2.01 ppm, and the second is a multiplet at -0.69 ppm. When butane gas was bubbled afterward through the same sample, isobutane was completely replaced by butane. However, when isobutane was bubbled again, isobutane does not replace butane. Thus, both peaks, butane and isobutane will be present.

The gas encapsulation takes place upon flushing the NMR sample with the corresponding gas using a long needle that will be inserted in to the bottom of the sample. The gas that is coming through the needle was stored in a balloon. The balloon is only used once for every sample and then it was disposed. The sample contains 2.0 mg of the solid sample and 0.6 ml of solvent for every trial.

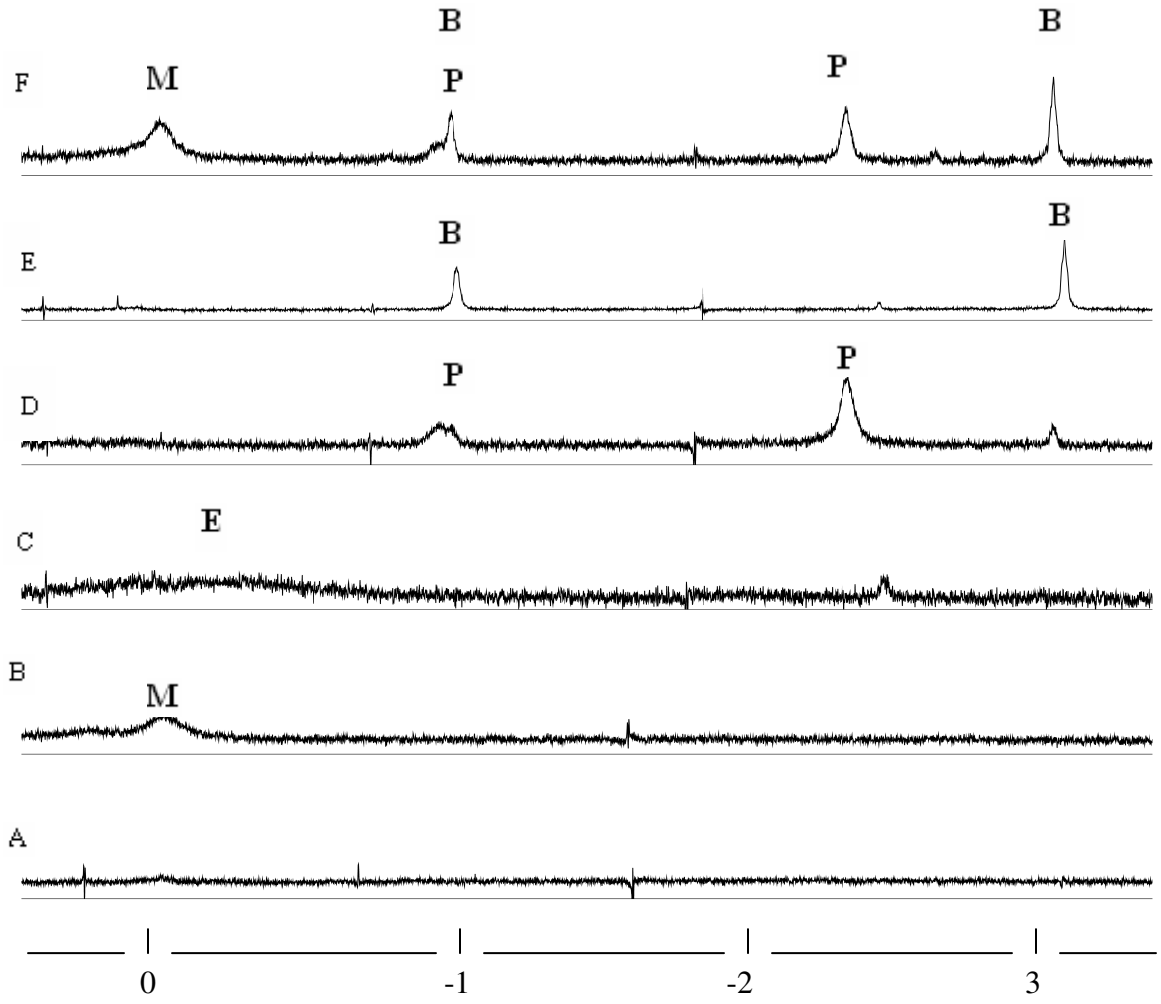

Figure 2.2 Gas encapsulation in hemicarceplex **4**. NMR Spectra (D_2O, pH 9, 500 MHz, rt) hemicarceplex **4**. A) empty hemicarcerand **4**; B) + methane; C) + ethane; D) + propane; E) + butane; F) + natural gas. Encapsulated gas is pointed out with corresponding letter. M = methyl, E = ethyl, P = Propane, B = Butane

2.3 Octaacid Hemicarcerand

To synthesize water soluble hemicarcerand **8**, hydroxyl cavitands **5**[10] were reacted with diesters **6**[12] in *N*-methyl-2-pyrrolidinone (NMP) **5** in the presence of Cs_2CO_3 to afford hemicarcerand **7**. The reaction took place under high dilution conditions because eight covalent bonds are made simultaneously. This also leads to lower yields. A hydrolysis reaction was used to convert the ester groups to carboxylic acids. This reaction takes place by reacting **7** with potassium hydroxide in the presence of 18-crown-6. After the removal of the organic layer solid **4** was obtained by adding 1 M HCl to the mixture. Upon the addition of a small amount of NaOH (~ pH 9), deprotonation of the acid groups results in the formation of a water soluble salt, **8**.

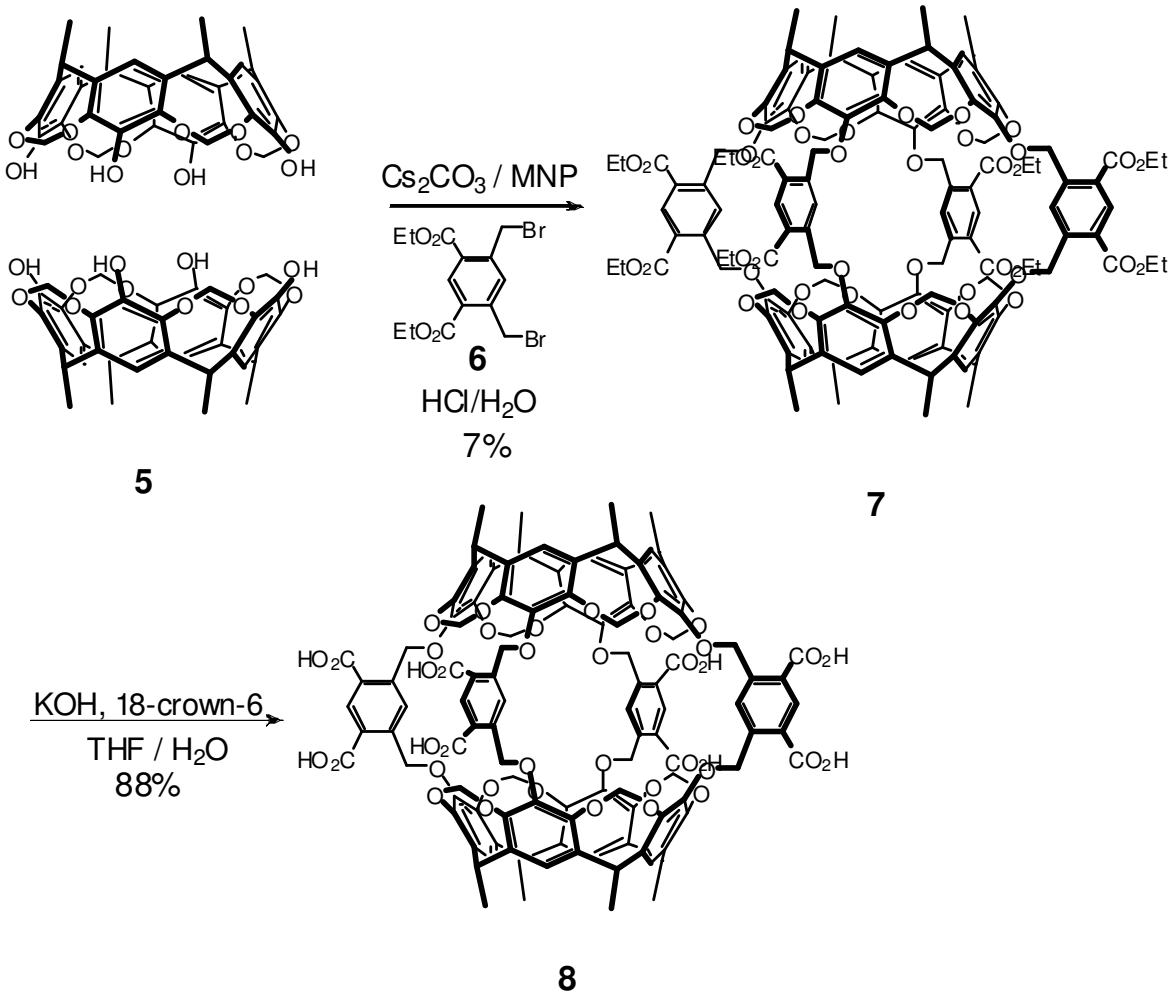

Scheme 2.2 The synthesis of water soluble tetrahemicarcerand **8**

As depicted in figure 2.3, one can notice that a signal appears upon the encapsulation of methane in hemicarcerand **8** at -0.40 ppm. Encapsulated ethane exhibited a broad peak around -0.15 ppm. Encapsulated propane showed two peaks, the first at -0.12 ppm and the second peak at -1.20 ppm. Encapsulated butane also showed two peaks: the first peak at -0.13 ppm and second peak at -2.07. However, when natural was bubbled in hemicarcerand **8** solution, only butane and few impurities were encapsulated. This is explained by the larger size cavity that **8** possess. Since larger size cavities favor guests of larger sizes, **8** is more selective toward the encapsulation of butane over smaller gases such as propane or ethane.

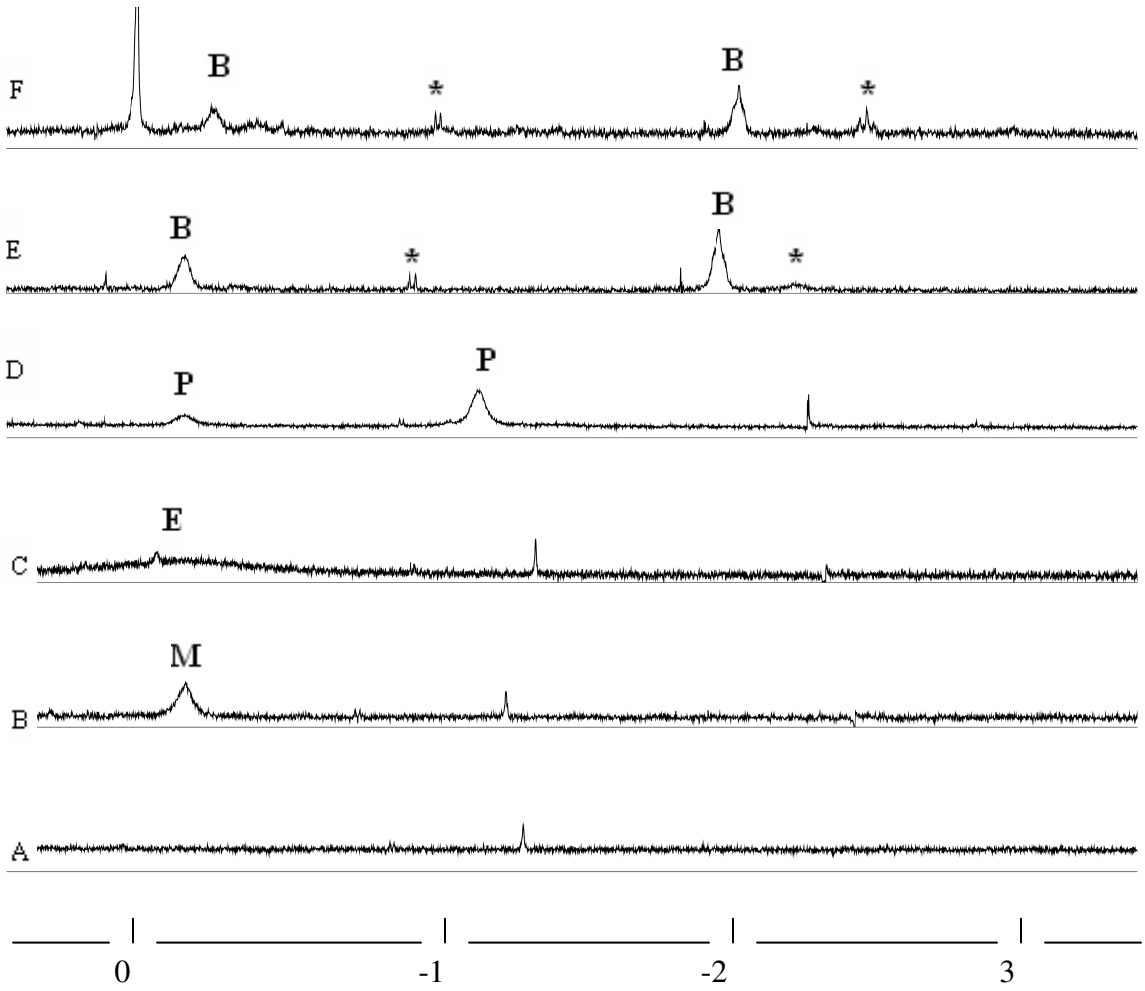

Figure 2.3 Gas encapsulation in hemicarceplex **8**. NMR Spectra (D_2O, pH 9, 500 MHz, rt) hemicarceplex **8**. A) empty hemicarcerand **4**; B) + methane; C) + ethane; D) + propane; E) + butane; F) + natural gas.Encapsulated gas is pointed out with the corresponding letter. Gas impurities possibly pentanes and hexanes are pointed out with (*). M = methyl, E = ethyl, P = Propane, B = Butane.

2.4 Discussion

When the NMR signals were integrated, a 1:1 stoichiometry in all cases was found. This allowed us to obtain the packing coefficients (PC), which is the ratio of the guest volume to the host volume.[13] The inner cavity of hemicarcerand **4** was found to be ~ 160 $Å^3$ using MM2 calculations. The obtained PCs are 18, 28, 39, and 49% for **4**·methane, **4**·ethane, **4**·propane, and **4**·butane, respectively. The inner cavity of hemicarcerand **8** was found to be ~ 180 $Å^3$. The obtained PCs are 16, 25, 35, and 44% for **8**·methane, **8**·ethane, **8**·propane, **8**·butane, respectively. From the literature, one can see that these values are relatively lower than the average 55% value observed for encapsulation of organic guests in solution.[13] However, it is found to be in agreement with the accepted molecular crystallography knowledge for gases.[14] Similar values of gas encapsulation in water were observed by others.[15]

In both cases, the guest size seems to play an important role in binding strength. This means that in addition to hydrophobic effects, CH-π and van der Waals forces are also at play. For larger gases, propane and butane, the signals of free and incarcerated molecules were seen separately, which indicates high exchange barriers. As an example, signals for free butane in D_2O for hemicarcerand **4** were seen at 1.30 (CH_2) and 0.90 (CH_3) ppm. The encarcerated butane showed signals at -1.20 (CH_2) and -3.37 (CH_3) ppm. This great difference in the chemical shift implies that the guest is aligned along the long north-south axis of **4**, and the alkyl protons appear under the shielding power of the resorcinarene aromatic rings.

It also appears that there is no rapid rotation of the guest around the east-west axis of **4** and **8** on the ^1H NMR time scale. However, when the smaller gases, methane and

ethane, were bubbled through the solution of **4** or **8**, faster in-and-out exchange processes were observed. For example, with methane in **4**, a broad peak centered at ~ 0 ppm appeared, which might represent the average chemical shift of free gas (0.16 ppm) in water and the value of its encapsulated species. In the case of ethane, an even broader, gently sloping peak at – 0.19 was observed in both cases. While the gas alkyl protons still appear to be somewhat shielded by the cavity aromatic rings, rapid rotation of the guest around the north-south and east-west axes most probably takes place.

It was also found that methane, ethane, and propane can easily replace each other in the inner cavity. For example, by flushing hemicarceplex **4**·propane with methane or ethane, the corresponding methane ethane complexes were generated. When propane is introduced again, complex **1**·propane was restored. These were repeated five times to give reproducible results. These are important observations since such exchange cycles cannot be easily achieved in conventional encapsulation studies with liquid and solid guests. On the other hand, hemicarceplex **4**·butane is very robust. To release the encarcerated butane the complex was heated at 100-125 °C under vacuum.

2.5 Conclusion

Comparing the data in both cases of our hemicarcerand, we conclude that hydrophobic interactions served as the primary force leading to encapsulation of hydrophobic gases in water. We believe that our findings can be used in the design of molecular containers for a variety of hydrophobic gases. The results might also be useful in contributing to explaining the mechanisms of biological trafficking of gases. Our goal for this project was primarily for separation, purification and storage of gases. There are a

number of water-soluble molecular containers for hydrophobic gases are known, they are formed via self-assembly and thus are stable only under specific conditions. In contrast, our hemicarcerands are quite robust. Therefore, they are relatively uneffected by the surrounding environment.

However, our systems have a few disadvantages. For example, the yields that we obtain are quite low. Therefore, these cavities will be more useful if they were to be synthesized in higher yields. With additional research, some of the critical steps might be optimized. For example, the coupling steps between the two cavitands. If that step was modified, these systems will be more applicable toward industry considerations.

CHAPTER 3

GAS ENCAPSULATION IN SOLID STATE

3.1 Background

The need for gas separation and purification is becoming more and more desirable. Materials that are used for gas purifications are limited in number and the need for new and more advanced material is always valuable. The area of nano- or microporous networks is becoming a major topic of study by many supramolecular chemists.[16] Examples of such porosity polymers are metal-organic microporous materials (MOMs) and metal-organic frameworks (MOFs). These systems have been designed for gas storage and transport.[17] MOMs and MOFs can adsorb many gases, e.g. O_2, Ar, CO_2, N_2O, H_2, CH_4, and more. Since MOFs are able to encapsulate H_2, they can be good candidates for vehicular hydrogen-based economy, which in turn interests the U.S. Department of Energy.[16]

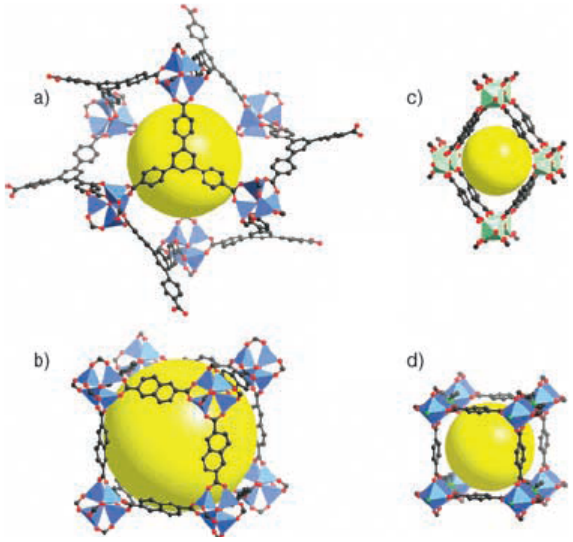

Figure 3.1 Examples of Metal Organic Frameworks (MOFs). a) MOF-177,$Zn_4O(btb)_4$ (btb = benzene-1,3,5-tribenzoate), b) IRMOF-8, $Zn_4O(ndc)_3$ (ndc = naphthalene-2,6-dicarboxylate), c) MIL-53, M(OH)(bdc) (M = Al^{3+} or Cr^{3+}),and d) Zn_2-$(bdc)_2$(dabco) (dabco = 1,4-diazabicyclo[2.2.2]octane).[17]

Another example of solid state encapsulation of gases is the use of the lattice voids of a crystalline calix[4]arene framework.[18] Atwood et al. demonstrated the ability of the framework to encapsulate CH_4, CF_4, C_2F_6, CF_3Br, and recently H_2 and NO_x gases.[23,24] Other examples of gas encapsulating polymers are covalent organic frameworks (COFs).[19] These materials are composed of expanded porous graphitic layers. Another similar example is a polymer with intrinsic microporosity (PIM), this polymer contains bowl shaped cyclotricatechylene cavities.[20]

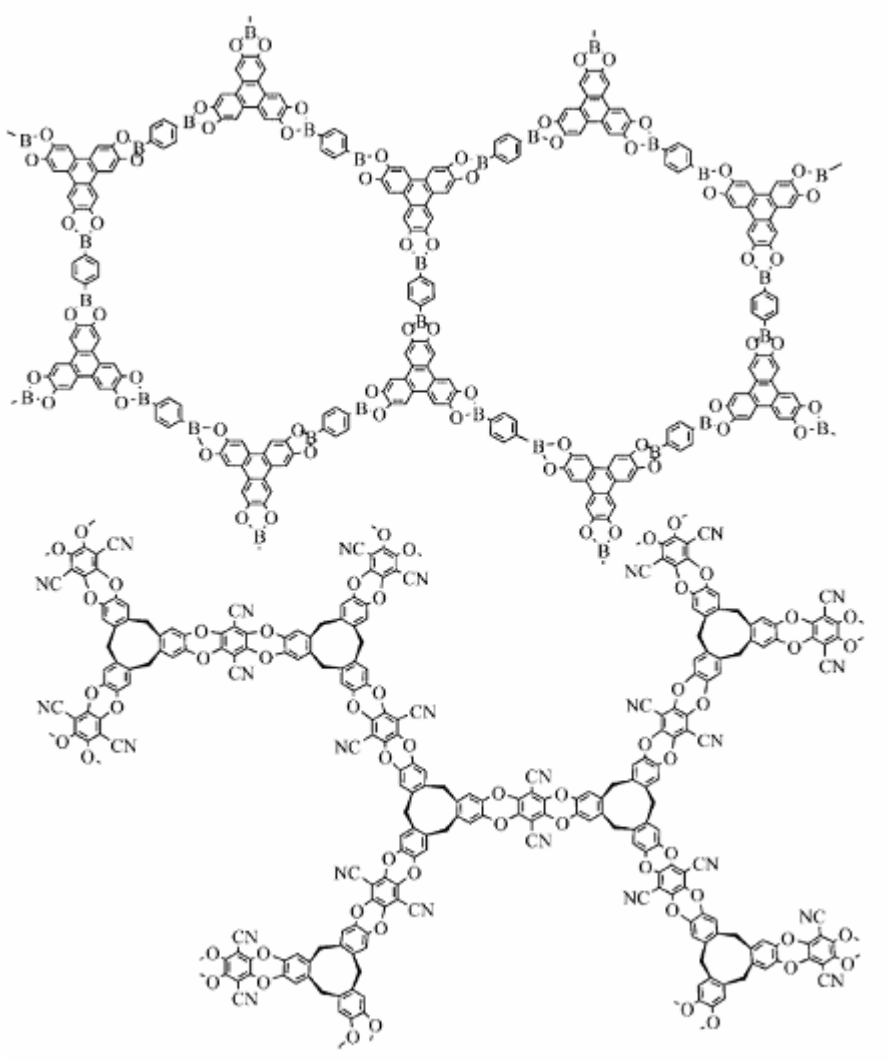

Figure 3.2 Example of covalent organic frameworks (COFs), top, and polymer with intrinsic microporosity (PIM), bottom.

These and many other metal coordinated polymeric complexes have been used as gas storing materials. However, the use of pure organic solids in which its building blocks are linked by covalent bonds are underdeveloped. This chapter will discuss the synthesis of the first cavity containing pure organic polymer. To illustrate the idea we synthesized solid polymeric materials from our hemicarcerand **4** and used commercially available butane and propane as our target guests.

From the literature, it was found that gas encapsulation in solid state was achieved by using simple hemicarcerand.[21] A slightly modified hemicarcerand possesses a large enough cavity to accommodate a benzene-size guest molecule.[22] Cram showed that CO_2, N_2, O_2, and Xe could also be encapsulated in chloroform. Therefore we tested our hemicarcerands for gas encapsulation in the solid state and took it a step further to synthesize the first hemicarcerand based polymer.

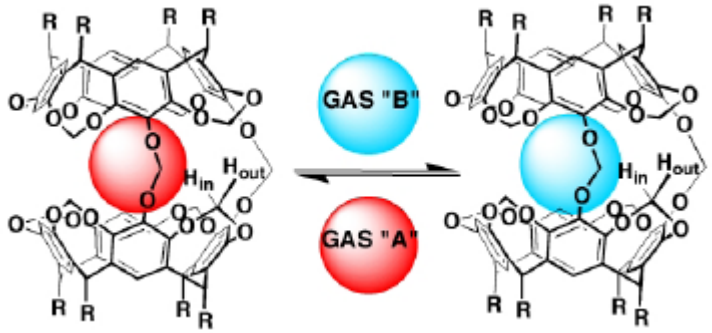

Figure 3.3 The reversible encapsulation of gases in solid state in traditional hemicarcerand.[21]

3.2 Gas Encapsulation in Water-Solid Interface

To illustrate the idea in its simplest form, solid hemicarcerand **4** was tested for gas encapsulation. Powdered hemicarcerand **4** was suspended in water (pH ~ 7) and flushed with butane for 30 minutes. The water solution was then flushed with N_2 for 15 min to remove any traces of butane in water. A small amount of NaOD was then added to dissolve the solid hemicarcerand. From (Fig 3.4) below, one can notice that new peaks appeared indicating the encapsulation of butane in **4**. Encapsulated butane showed two peaks, first peak at -1.13 ppm and second peak at -3.40 ppm.

Gas encapsulation in only the solid state showed similar results. This was done by placing solid hemicarcerand **4** in an NMR tube. It was then flushed with butane gas for 10 minutes using a long needle. The solid was then flushed with nitrogen gas to remove any butane between crystals. Deuterated water was added to the tube and it was also flushed with nitrogen gas. The solid sample was then dissolved by adding 1μL of 10 M NaOD in D_2O. Spectra similar to the one below were obtained.

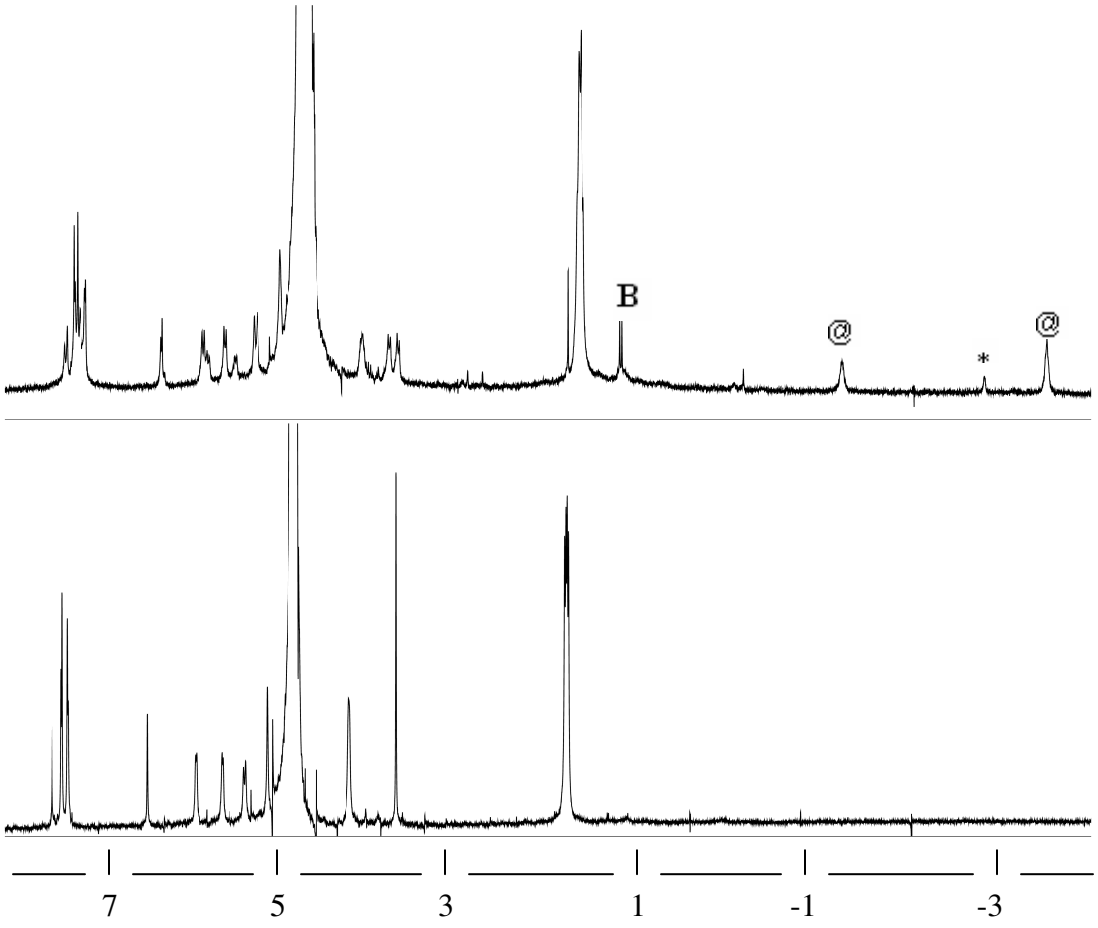

Figure 3.4 Gas encapsulation in water-solid interface. Bottom, empty hemicarcerand **4**. Top, butane encarcerated in **4** shown by (@). Free butane is shown with (B). Sample impurities are shown with (*).

Encapsulations of gases in heterogeneous mixtures using solid hemicarcerands in water led us to believe that a polymeric material of these cavities may posses some of the same properties. Therefore, we prepared the first hemicarcerand polymer.

3.3 Solid Encapsulation of Gases

To check the ability of our monomer unit to encapsulate gases, solid hemicarcerand **3** was flushed with butane. It was then flushed with N_2 to remove any butane residue between crystals. The solid was then dissolved in deuterated benzene. If butane was encapsulated, it will leave the cavity and appear as free butane in the ^1H NMR spectra.

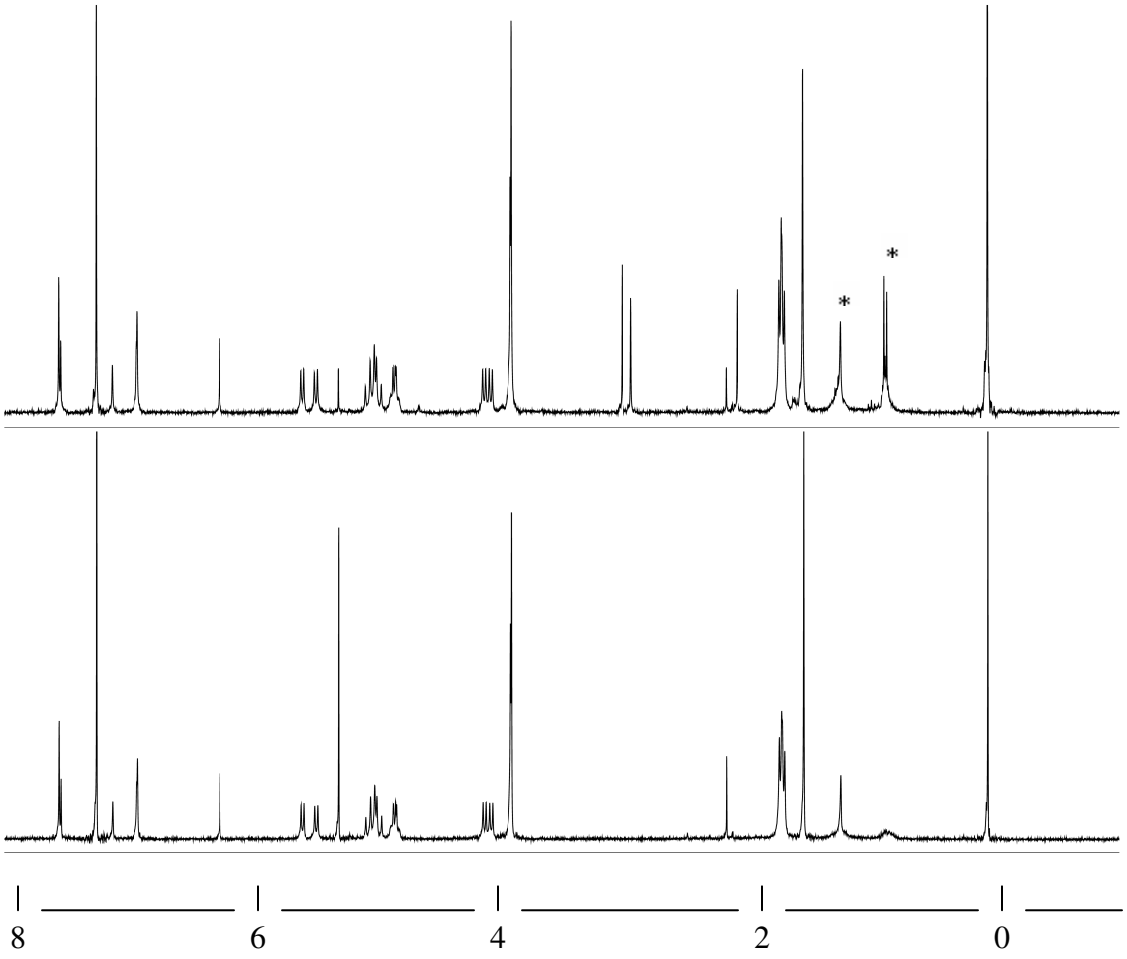

Figure 3.5 Gas encapsulation in solid monomer hemicarcerand **4**. ^1H NMR Spectra (Benzene-d_6, 300 MHz, rt). Bottom, carcerand **3** before butane. Top, previously encapsulated butane is shown as free butane (*) after flushing in solid state.

As expected, free butane appeared in the spectra suggesting the ability of solid hemicarcerand to encapsulate the gas even in solid state. Therefore, we prepared the corresponding polymeric material. Each portal of the hemicarcerand contains a diester group that was utilized as a connection site between hemicarcerand units. The diesters from each portal were coupled with an amino group from the connecting bridge to give a cyclic imide.

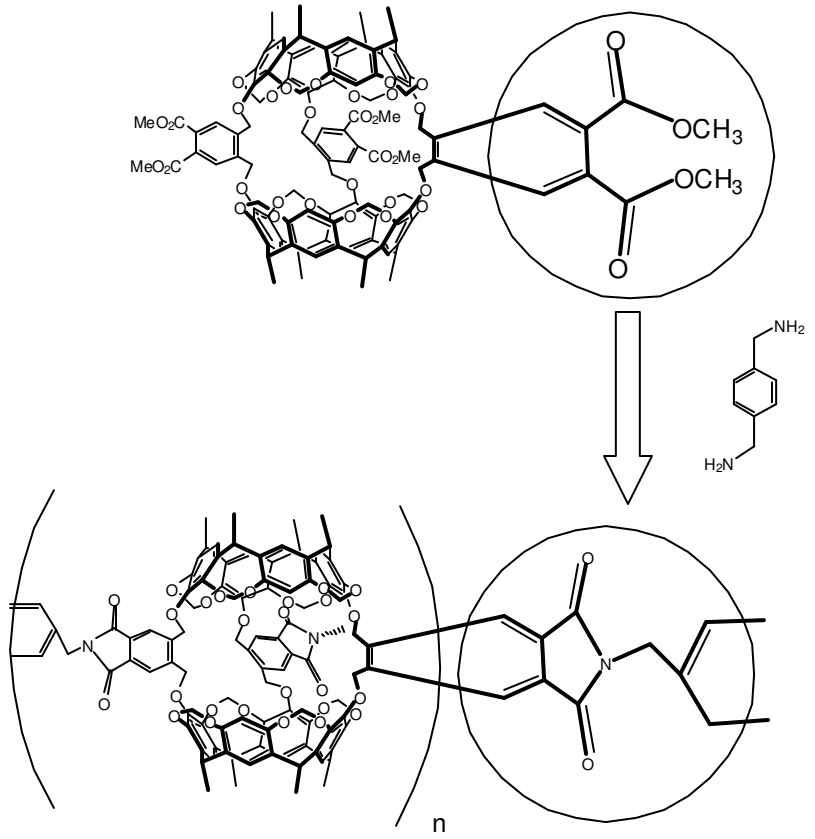

Figure 3.6 A magnification of the functional groups used in the polymerization process going to the final product, the cyclic imide.

3.4 Model Reaction

Since the yield of our hemicarcerand from its preparation is not high, it was in our best interest to find the reaction condition that produced the highest yield first. To find

the best conditions for our polymerization, a model reaction was performed. We chose dimethyl phthalate as our model since it closely resembles the outer side of our hemicarcerand portals. Upon finding the best conditions we moved into the synthesis of the first example of hemicarcerand polymer.

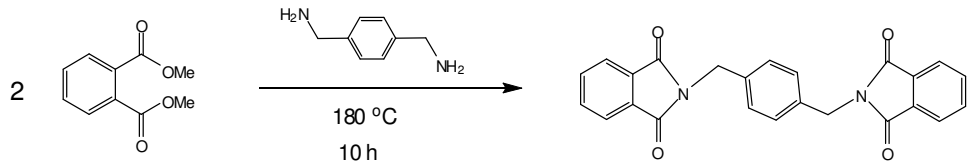

Scheme 3.1 Model reaction and cyclic imide synthesis.

The model dimer was synthesized by adding two equivalents of dimethyl phthalate to one equivalent of *p*-xylylenediamine. The mixture was left for 10 hours at 180 °C. No solvents or other reagents were used. The product was analyzed by ^{1}H NMR and FT-IR. It was found that the conditions stated above resulted in the synthesis of the desired cyclic imide dimer between two dimethyl phthalate and one *p*-xylylenediamine. These neat reaction conditions were the one used to synthesize our hemicarcerand polymer.

3.5 Synthesis of Polymer

The polymer was synthesized by connecting hemicarcerands by their portals. The reaction took place by placing 1 equivalent of hemicarcerand **3** to 1.5 equivalents of *p*-xylylenediamine. The mixture was left for 10 hours at 180 °C. No solvents or other reagents were used. The color of the solid turned pale yellow and it became insoluble in organic solvents. The solid was then washed with benzene and left to dry at 180 °C under vacuum.

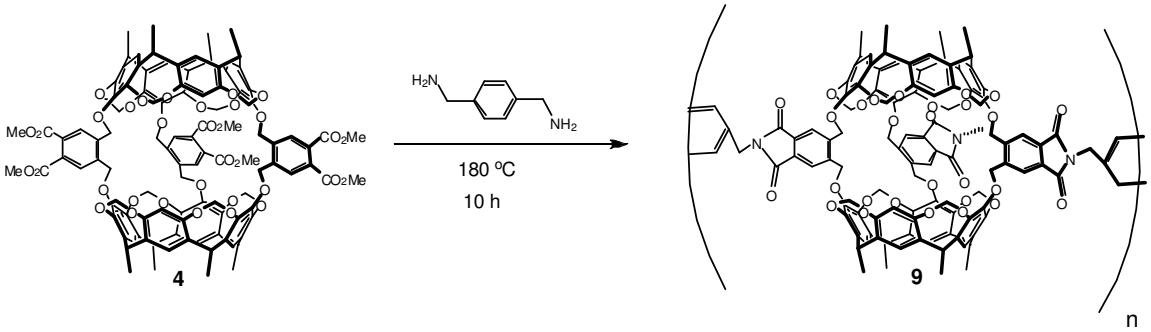

Scheme 3.2 The synthesis of the hemicarcerand polymer.
A proposed structure for the polymeric material was done using MM2 Force Field molecular modeling.

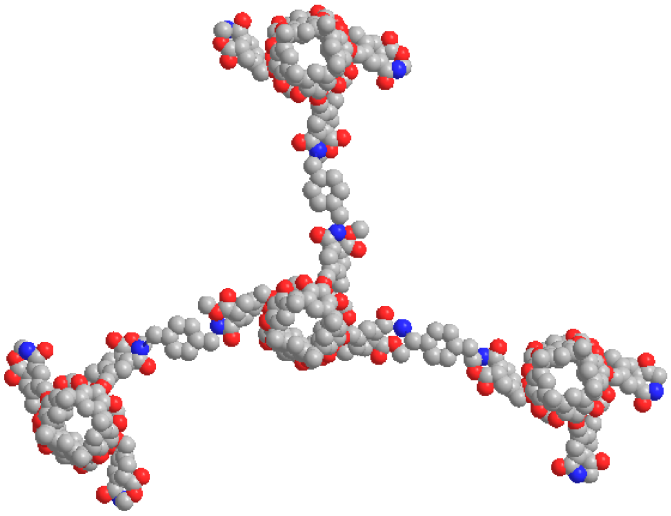

Figure 3.7 Molecular modeling of polymer.

The polymer was characterized by elemental analysis and FT-IR. In the literature, it was found that cyclic imide has a distinct band around 1770 cm^{-1}.[25] The band was observed in the IR spectra of our model reaction as well as in our polymer.

a)

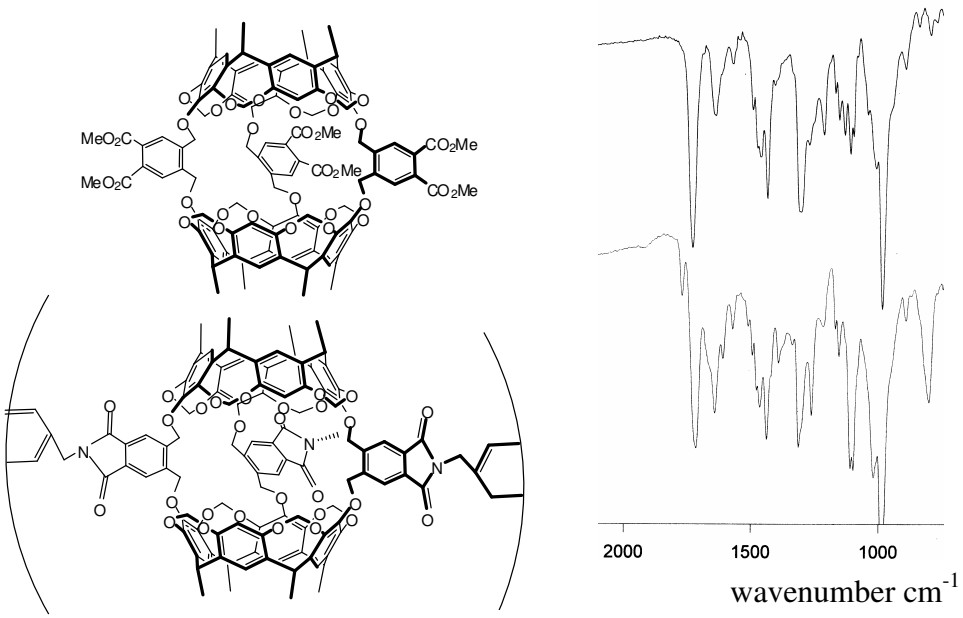

b)

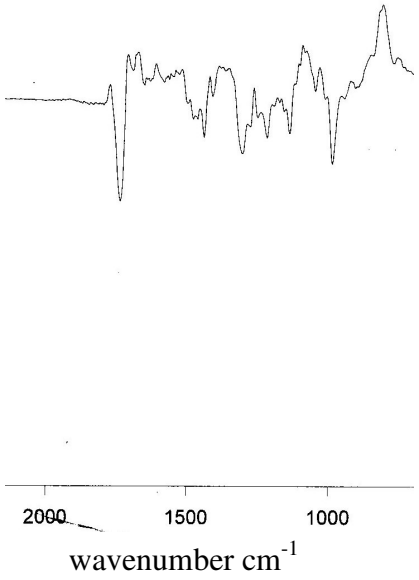

Figure 3.8 IR spectrum of the polymer. a) The change in the IR spectra going from hemicarcerand (top) to polymer (bottom) b) The difference between the two spectra in (a).

3.6 Encapsulation of Gases

Gas encapsulation took place by flushing butane or propane over the polymer. The solid polymer was flushed with N_2. The saturated solid was then be suspended in deuterated benzene. Any encapsulated butane or propane will then leave the cavity and show as free gas in the ^{1}H NMR spectra. The experiment was repeated five times to show reproducibility. Since our polymer is insoluble in benzene, the benzene spectra will show no sign of it. As soon as the gas guest leaves the cavity, only it will be visible in the spectra.

Another special property of our polymer is its ability to be recycled and reused. After the encapsulation, the complex can be placed at a 180 °C under vacuum for 10 hours to regenerate the empty polymer. If the recycled polymer was placed in benzene, no sign of previously encapsulated guest is shown in the ^{1}H NMR spectra. We believe this to be a unique and important property for such a gas encapsulating solid. The figure below illustrates the cycle of butane inside the polymer solid.

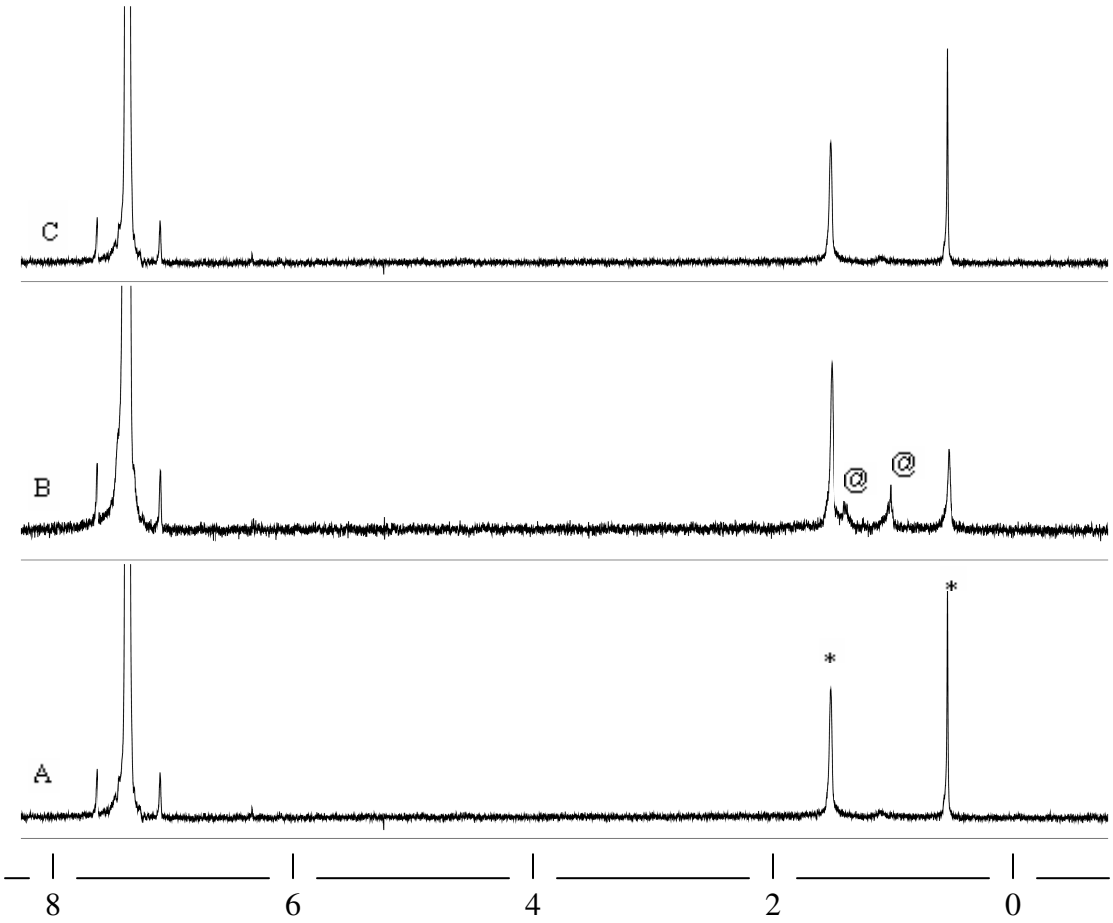

Figure 3.9 Butane cycle in polymer. NMR Spectra (Benzene-d_6, 300 MHz, rt). A) empty polymer (insoluble) **8**, B) + butane (@), C) regeneration of empty polymer by removing butane. Impurities are shown with (*)

To explain the cycle, empty polymer was suspended in deuterated benzene (Figure 3.9A). The benzene was then removed and the polymer was dried completely at a 180°C for 10 hours under vacuum. The solid polymer was then flushed with butane then with N_2. It was then suspended in deuterated benzene (Figure 3.9B). The benzene was then removed and the solid polymer was dried. The dry polymer was then suspended in deutrated benzene (Figure 3.9C). Propane was also used and similar results were obtained.

3.7 TGA Analysis

To further characterize gas encapsulation in the polymer a thermogravimetric analysis (TGA) study was done with the idea to look for two steps in the mass/temp plot. The first one corresponds to a change in weight of the complex upon the loss of encapsulated gas. The second one corresponds to the decomposition of the polymer. It was expected that the encapsulated gas would appear later in the analysis due to having it tightly bound inside the cavity, which in turns requires more energy to release it.

The experiment was done with three different samples, prepared under different conditions. The first experiment was analyzing the polymer in its empty state. This was done by placing the polymer in a 120 °C oil bath under vacuum (Fig 3.10A). The only step present in the spectrum is the one responsible for the decomposition of the polymer which begins at 300 °C and ends at 500 °C. The second experiment was flushing the polymer with butane for 10 min then flushing it with N_2 gas for 5 min (Fig 3.10B). As shown in the spectrum, only the decomposition of the polymer step 300-500 °C is present. There is no sign of another step which suggests that butane is not incorporated in the cavity of the polymer. The third experiment was preformed by flushing the polymer with butane gas for 10 min **without** flushing it with N_2 gas afterwards (Fig 3.10C). This last spectrum shows two steps, one for the loss of (presumably) butane 50-88 °C, the second was the decomposition of the polymer 300-500 °C.

The spectra in (Fig 3.10) suggest that butane gas is entrapped within the crystals of the polymer rather than encapsulated in the cavity. In the third experiment, the butane saturated polymer was not flushed with N_2. Therefore, the butane gas that was within the polymer crystals lattices was the one responsible for the first step in Fig (3.10C). If

butane gas was encapsulated in the cavity, it might be anticipated that more energy will be needed to remove it. However, the TGA analysis did not show the any steps that can conclusively be shown to correspond to the loss of any encapsulated butane.

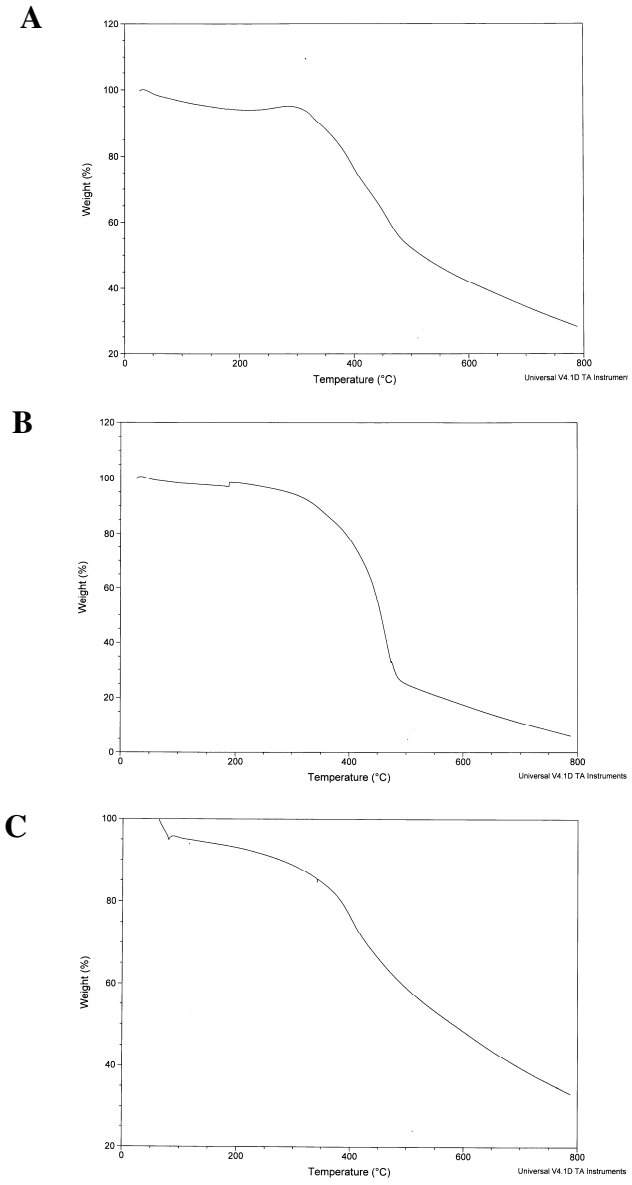

Figure 3.10 TGA Analysis of gas encapsulation in polymer. A) Empty polymer; B) Polymer flushed with butane then N_2; C) Polymer flushed with butane but not with N_2.

CHAPTER 4

EXPERIMENTAL DETAILS

General. Melting points were determined on a Mel-Temp apparatus (Laboratory Devices, Inc.) and are uncorrected. ^{1}H, ^{13}C NMR, and COSY NMR spectra were recorded at 295 ± 1 K on JEOL 300 and 500 MHz spectrometers. Chemical shifts were measured relative to residual non-deuterated solvent resonances. FTIR spectra were recorded on a Bruker Vector 22 FTIR spectrometer. ESI-TOF high-resolution mass spectra were recorded on an Agilent ESI-TOF mass spectrometer at the Scripps Center for Mass Spectrometry (La Jolla, CA). Elemental analysis was performed on a Perkin-Elmer 2400 CHN analyzer. All experiments with moisture- and/or air-sensitive compounds were performed under a dried nitrogen atmosphere. All reagents were purchased from Sigma-Aldrich (St. Louis, MO) and AK Scientific (Mountain View, CA) and were used as received.

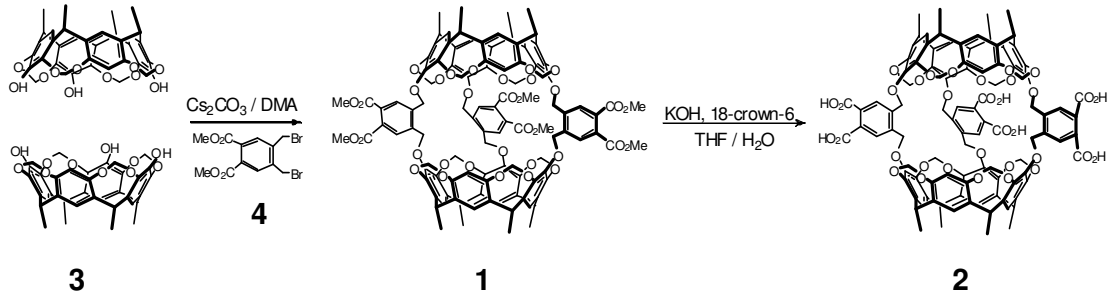

3 **4** **1** **2**

Preparation of hemicarcerand 1: To a suspension of cesium carbonate (2.34 g, 7.20 mmol) in dry dimethylacetamide (DMA) (200 mL) at room temperature was added dropwise a solution of triol **3**[1] (0.20 g, 0.31 mmol) and diester **4**[2] (0.20 g, 0.53 mmol) in DMA (20 mL) over 16 h. After the reaction mixture was stirred at 40 °C for 48 h, the solvent was evaporated in vacuo and the residue was treated with 30 mL of 1N HCl. Undissolved material was filtered, washed with water and then dissolved in a small amount of $CHCl_3$. After treatment with methanol, the formed precipitate was filtered, dried and purified by chromatography on a column of silica gel using first CH_2Cl_2 and then 2% of acetone in CH_2Cl_2 as the mobile phase. The isolated hemicarcerand **1** was dissolved in a small amount of chloroform and diluted with methanol. The resulting precipitate was filtered and dried under vacuum at 120 °C to give pure **1**, (0.019 g, 0.0098 mmol, 6%); m.p. >300 °C (decomp.); ^{1}H NMR (500 MHz, $CDCl_3$): δ 7.56 (s, 4H), 7.54 (s, 2H), 7.12 (s, 2H), 6.93 (s, 2H), 6.92 (s, 4H), 6.26 (s, 2H), 5.59 (d, 4H, *J* = 7.2 Hz), 5.48 (d, 4H, *J* = 7.2 Hz), 5.01 (m, 12H), 4.85 (m, 8H), 4.12 (d, 4H, *J* = 7.2 Hz), 4.07 (d, 4H, *J* = 7.2 Hz), 3.91 (s, 6H), 3.90 (s, 12H), 1.72 (m, 24H); MS (ESI-TOF high acc.) for [MH^+]: calcd: 1935.5699, found: 1935.5697.

Preparation of hemicarcerand 2: To a solution of hemicarcerand **1** (0.0180 g, 0.0098 mmol) in THF (1 mL) was added 1M KOH (1 mL) and 18-crown-6 (0.003 g, 0.011 mmol). The reaction mixture was vigorously stirred at 80 °C for 8 h. THF was removed under vacuum and an extra 3 mL of 1M KOH was added. The solution was filtered through a glass wool plug to remove undissolved impurities. The filtrate was acidified to pH 1 (pH paper) with 1M HCl and the thus formed precipitate was filtered and washed five times with water. After drying under vacuum at 120 °C, pure hemicarcerand **2** (0.015 g, 0.0081 mmol, 83%) was obtained: m.p. >300 °C (decomp.); ^{1}H NMR (500 MHz, D_2O, pH 9, NaOD) δ 7.47 (s, 2H), 7.37 (s, 2H), 7.36 (s, 4H), 7.30 (s, 4H), 7.29 (s, 2H), 6.41 (s, 2H), 5.88 (d, 4H, *J* = 7.2 Hz), 5.59 (d, 4H, *J* = 7.2 Hz), 5.36 (d, 4H, *J* = 11.6 Hz), 5.09 (s, 4H), 4.90 (m, H, overlap with H_2O), 4.184 (br s, 8H), 1.79 (m, 24H); MS (ESI-TOF high acc.) for $[M-H]^-$: calcd: 1849.4615, found: 1849.4607.

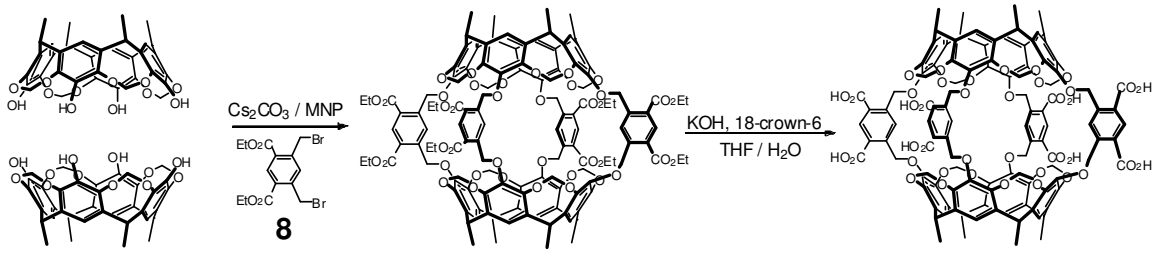

7 **8** **5** **6**

Preparation of hemicarcerand 5: To a suspension of cesium carbonate (3.13 g, 9.6 mmol) in dry *N*-methyl-2-pyrrolidinone (NMP) (200 mL) was added solution of tetrol **7**[1] (0.3 g, 0.457 mmol) and diester **8**[2] (0.391 g, 0.959 mmol) in NMP (20 mL) dropwise over 16 h. Another 20 mL solution of diester **8** (0.124 g, 0.305 mmol) was then added. After,

the reaction mixture was stirred at 40 °C for 48 h, the solvent was evaporated in vacuo and the residue was treated with 30 mL of 1N HCl. Undissolved material was filtered, washed with water and then dissolved in a small amount of $CHCl_3$. After treatment with methanol the resulting precipitate was filtered, dried and purified by chromatography on a column of silica gel using first CH_2Cl_2 and then 2% acetone in CH_2Cl_2 as the mobile phase. The isolated hemicarcerand **5** was dissolved in small amount of chloroform and diluted with methanol. The thus formed precipitate was filtered and dried under vacuum at 120 °C to give pure **5** (0.015 g, 7.1 % yield). ^{1}H NMR (500 MHz, $CDCl_3$): δ 8.56 (s, 4H), 8.46 (s, 4H), 7.19 (s, 16 H), 6.90 (s, 8 H), 5.46 (d, 8H, J = 7.2 Hz), 5.29 (s, 16H), 4.79 (q, 8H, J_1 = 7.2 Hz, J_2 = 14.9 Hz), 4.20 (q, 16H, J_1 = 7.2 Hz, J_2 = 14.9 Hz), 4.18 (d, 8H, J = 7.2 Hz), 1.64 (d, 24H, J = 7.12 Hz), 1.29 (t, 24H, J = 7.2 Hz). Characterization data matched published literature.[26]

Preparation of hemicarcerand 6: To a solution of hemicarcerand **5** (0.018 g, 0.0098 mmol) in 1 mL of THF was added 1M KOH (1 mL) and 18-crown-6 (0.003 g, 0.011 mmol). The reaction mixture was vigorously stirred at 80°C for 8 hr. THF was removed under vacuum and an extra 3 mL of 1M KOH was added. The solution was filtered through a glass wool plug to eliminate undissolved impurities. The filtrate was acidified to pH 1 with 1M HCl and formed precipitate was washed several times with water in a centrifuge tube. After drying under vacuum at 120 °C, pure hemicarcerand **6** (0.012 g, 88% yield). ^{1}H NMR (500 MHz, D_2O, pH 9, NaOD) δ 7.88 (s, 4H), 7.59 (s, 4H), 7.22 (s, 8H), 5.46 (d, 8H, J = 7.4 Hz), 5.09 (s, 8H), 4.21 (d, 8H, J = 7.4 Hz), 3.55 (s, 4H), 1.62 (d, 24H, J = 7.4). Characterization data matched published literature.[26]

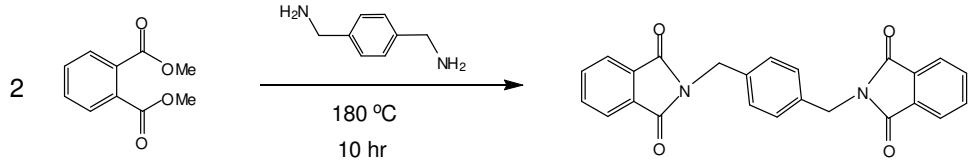

2,2'-(1,4-phenylenebis(methylene))diisoindoline-1,3-dione: To a solution of dimethyl phthalate (0.20 g, 1.03 mmol) in 0.5 mL of chloroform was added *p*-xylylenediamine (0.10 g, 0.73 mmol). The chloroform was removed under vacuum and the reaction mixture was vigorously stirred at 180 °C for 12 h. After drying under vacuum at 180 °C, the pure complex (0.25 g, 86%) was obtained: ^{1}H NMR ($CDCl_3$, 300 MHz) δ 7.82 (m, 4 H), 7.69 (m, 4 H), 7.31 (s, 4 H), 4.79 (s, 4 H). FTIR (KBr, cm^{-1}) ν 1768, 1710 (C=O), 1395, 1341.

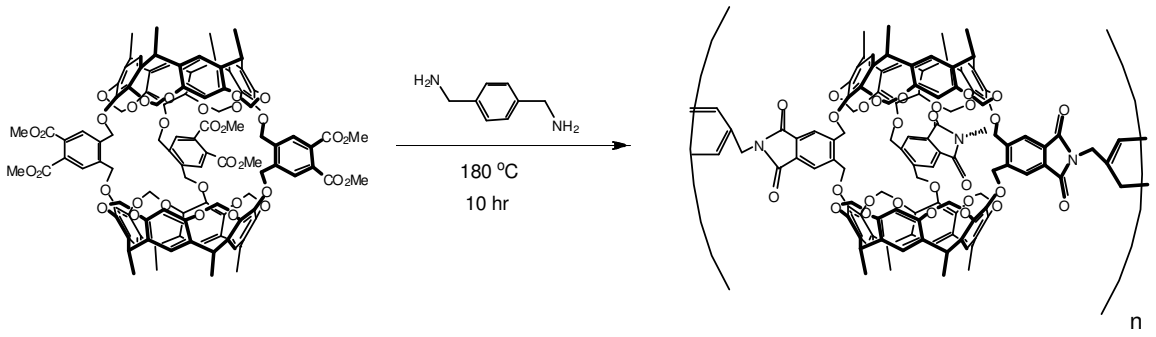

Synthesis of Polymer: To a solution of hemicarcerand **1** (0.010 g, 0.0052 mmol) in 0.5 mL of chloroform was added *p*-xylylenediamine (0.0066 g, 0.049 mmol). The chloroform was removed under vacuum and the reaction mixture was vigorously stirred at 180 °C for 12 h. The resulting solid was washed with benzene to remove excess *p*-xylylenediamine. After drying under vacuum at 180 °C, polymer (0.008 g, 59%) was obtained. FTIR (KBr,

cm^{-1}) ν 1773, 1710 (C=O), 1642, 1433, 1312, 1104, 982. Anal. Calcd. for $C_{111}H_{97}N_3O_{28}$: C, 68.76; H, 5.15; N, 2.97. Found: C, 66.81; H, 5.09; N, 3.14.

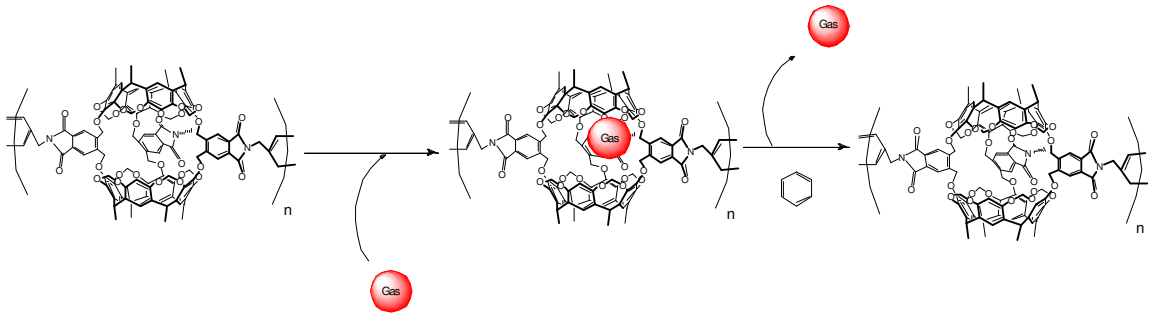

Encapsulation of Butane in Polymer: Over the solid polymer (2 mg) in an NMR tube, pure butane (>99.9%) was bubbled for 30 min. The solid was then flushed with N_2 for 15 min to remove any residue of butane between crystals. To the solid, 0.6 ml of deuterated benzene was added. The mixture was vigorously mixed. Solid precipitated at the bottom. Butane gas peaks appeared in the NMR spectrum indicating the ability of the polymer to encapsulate gases in solid state.

Encapsulation of Butane in Monomer Hemicarcerand: Over solid hexaester hemicarcerand **1** (2 mg) in an NMR tube, pure butane (>99.9%) was flushed for 30 min. The solid was then flushed with N_2 for 15 min to remove any residue of butane between crystals. To the solid, 0.6 ml of deuterated benzene was added. The mixture was vigorously mixed. Butane gas peaks appeared in the NMR spectrum indicating the ability of the monomer to encapsulate gases in solid state.

Encapsulation of Butane in Solid Hemicarcerand in Water: Solid hexaacid hemicarcerand **2** (2 mg) was placed in an NMR tube with 0.6 mL of D_2O. The suspention

was flushed with pure butane (>99.9%) for 30 min. N_2 was then bubbled for 15 min to remove any residue of butane in D_2O. 40 wt % NaOD in D_2O (1 μL) was added to the mixture to dissolve the hexaacid hemicarcerand resulting in ~ pH 9 solution . Butane gas peaks appeared in the negative region of the NMR spectra indicating the ability of the monomer to encapsulate gases in solid-water interface.

REFERENCES

(1) Lehn J. M. *Science* **1993***, 260,* 1762-1763.

(2) Oshovsky G. V; Reinhoudt D. N; Verboom W. *Angew . Chem., Int. Ed.* **2007,** *46*, 2366-2393.

(3) Rudkevich, D. M. Angew. *Chem., Int. Ed.* **2004**, *43*, 558-571.

(4) Rudkevich, D. M.; Leontiev, A. V. *Aust. J. Chem.* **2004**, *57*, 713-722.

(5) Rowsell, J. L. C.; Yaghi, O. M. *Angew. Chem., Int. Ed.* **2005**, *44*, 4670-4679.

(6) Rebek, J., Jr. *Acc. Chem. Res.* **1999**, *32*, 278-286.

(7) Atwood, J. L.; Leonard, J. B.; Agoston, J. *Angew. Chem., Int. Ed.* **2004**, *43*, 2948-2950.

(8) Hydrocarbon gases have very low solubility in water (1-2 mmol/L); see: McAuliffe, C. *J. Phys. Chem.* **1966**, *70*, 1267-1275.

(9) Encapsulation of hydrocarbon gases: (a) Gibb, C. L. D.; Gibb, B. C. *J. Am. Chem. Soc.* **2006**, *128*, 16498-16499. (b) Nakazawa, J.; Mizuki, M.; Shimazaki, Y.; Tani, F.; Naruta, Y. *Org. Lett.* **2006**, *8*, 4275-4278. (c) Nakazawa, J.; Nagiwara, J.; Mizuki, M.; Shimazaki, Y.; Tani, F.; Naruta, Y. *Angew. Chem., Int. Ed.* **2005**, *44*, 3744-3746. (d) Miyahara, Y.; Abe, K.; Inazu, T. *Angew. Chem., Int. Ed.* **2002**, *41*, 3020-3023. (e) Bartik, K.; Luhmer, M.; Dutasta, J. P.; Collet, A.; Reisse, J. *J. Am. Chem. Soc.* **1998**, *120*, 784-791. (f) Branda, N.; Wyler, R.; Rebek, J., Jr. *Science* **1994**, *263*, 1267-1268.

(10) Fraser, J. R.; Borecka, B., Trotter, J.; Sherman, J. C. *J. Org. Chem.* **1995**, *60*, 1207-1213.

(11) Wood, J. H.; Perry, M. A; Tung, C. C. *J. Am. Chem. Soc.* **1950**, *72*, 2989-2991

(12) Schroder, A.; Karbach, D.; Guther, R.; Vogtle, F. *Chem. Ber*. **1992**, *125*, 1881-1887

(13) Mecozzi, S.; Rebek, J., Jr. *Chem-Eur. J.* **1998**, *4*, 1016-1022.

(14) Kitaigorodsky, A. I. *Molecular Crystals and Molecules*; Academic Press: New York, **1973**, 18-19.

(15) Shivanyuk, A.; Scarso, A.; Rebek, J., Jr. *Chem. Commun.* **2003**, *11*, 1230-1231.

(16) Rudkevich, D. M. *Eur. J. Org. Chem.* **2007**, *20*, 3255-3270.

(17) a) James, S. L. *Chem. Soc. Rev.* **2003**, *32*, 276–288; b) Janiak, C. *Dalton Trans.* **2003**, 2781–2804; c) Rosi, N. L.; Eckert, J.; Eddaoudi, M.; Vodak, D. T.; Kim, J.; O'Keeffe, M.; Yaghi, O. M. *Science* **2003**, *300*, 1127–1130; d) Pan, L.; Sander, M. B.; Huang, X.; Li, J.; Smith, M.; Bittner, E.; Bockrath, B.; Johnson, J. K. *J. Am. Chem. Soc.* **2004**, *126*, 1308–1309; e) Düren, T.; Sarkisov, L.; Yaghi, O. M.; Snurr, R. Q. *Langmuir* **2004**, *20*, 2683–2689; f) Kitagawa, S.; Kitaura, R.; Noro, S. *Angew. Chem. Int. Ed.* **2004**, *43*, 2334–2375; g) Matsuda, R.; Kitaura, R.; Kitagawa, S.; Kubota, Y.; Belosludov, R. V.; Kobayashi, T. C.; Sakamotoo, H.; Chiba, T.; Takkata, M.; Kawazoe, Y.; Mita, Y. *Nature* **2005**, *436*, 238–241.

(18) Atwood, J. L.; Barbour, L. J.; Jerga, A. *Science* **2002**, *296*, 2367–2369.

(19) Cote, A. P.; Benin, A. I.; Ockwig, N. W.; O'Keeffe, M.; Matzger, A. J.; Yaghi, O. M. *Science* **2005**, *310*, 1166–1170.

(20) a) McKeown, N. B.; Ghanem, B. S.; Msayib, K. J.; Budd, P. M.; Tattershall, C. E.; Mahmood, K.; Tan, S.; Book, D.; Langmi, H. W.; Walton, A. *Angew. Chem., Int. Ed.*

2006,*45*, 1804–1807; b) McKeown, N. B.; Budd, P. M.; Msayib, K. J.; Ghanem, B. S.; Kingston, H. J; Tattershall, C. E.; Makhseed, S.; Reynolds, K. J.;. Fritsch D. *Chem-Eur. J.* **2005**, *11*, 2610–2620.

(21) Leontiev, A. V.; Rudkevich, D. M. *Chem. Commun.* **2004**, 1468–1469.

(22) a) Cram, D. J.; Tanner M. E.;. Knobler, C. B *J. Am. Chem. Soc.*, **1991**, *113*, 7717-7727; b) Paek, K.; Joo, K.; Kwon, S.; Ihm, H.; Kim, Y. *Bull. Korean Chem. Soc.*, **1997**, *18*, 80.

(23) a) Thallapally, P. K.; Lloyd, G. O.;. Wirsig, T. B; Bredenkamp, M. W.; Atwood, J. L.; Barbour, L. J. *Chem. Commun.* **2005**, 5272–5274; b) Thallapally, P. K.; Wirsig, T. B.; Barbour, L. J.; Atwood, J. L. *Chem. Commun.* **2005**, 4420–4422; c) Thallapally, P. K.; Dobran'ska, L.; Gingrich, T. R.; Wirsig, T. B.; Barbour, L. J.; Atwood, J. L. *Angew. Chem. Int., Ed.* **2006**, *45*, 6506–6509; d) Thallapally, P. K; McGrail, B. P.; Atwood, J. L. *Chem. Commun.* **2007**, 1521–1523.

(24) Dalgarno, S. J.; Thallapally, P. K., Barbour, L. J.; Atwood, J. L. *Chem. Soc. Rev.* **2007**, *36*, 236–245.

(25) Stamboliyska, B. A.; Binev, Y. I.; Radomirska, V. B.; Tsenov, J. A.; Juchnovski, I. N. *J. Mol. Struct.* **2000**, *516*, 237-245.

(26) Yoon, J.; Cram, D. J. *Chem. Commun.* **1997**, *5*, 497-498.

BIOGRAPHICAL INFORMATION

Anas Saleh was born in Zarqa, Jordan. He immigrated to the United States in October of 1998. He graduated high school from East Chicago Central High School in East Chicago, Indiana. He earned a Bachelor of Science degree in Biology and a Minor in Chemistry from Indiana University Bloomington in 2005 before attending the University of Texas at Arlington for graduate school.